Explosion Performance of Al Powder−Liquid Fuel Mixtures under Different Ambient Conditions

Jian Yao,* Chunhua Bai, and Chi Zhang
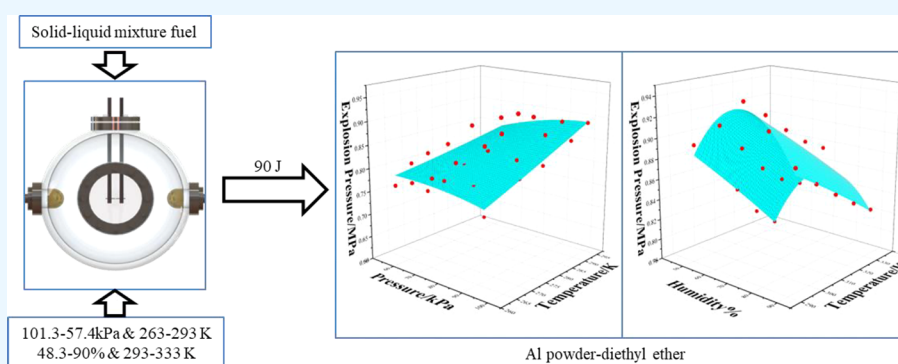
Read Online

ACCESS | Metrics & More | Article Recommendations

Al powder-diethyl ether

ABSTRACT: The explosion performance of Al powder−diethyl ether (A−D) and Al powder−diethyl ether−nitromethane (A−D−N) mixtures under low-temperature and low-pressure as well as high-temperature and high-humidity conditions were investigated in a 20 L explosion vessel. The explosion pressure, maximum pressure rise rates, and lower flammability limit (LFL) of the mixtures under binary ambient conditions were obtained. The results showed that the A−D−N mixture had a higher explosion pressure and LFL under the same ambient condition due to the addition of nitromethane. The explosion pressure and LFL of the A−D−N mixture had lower sensitivity to the variation of ambient parameters. The result could further help in explosion performance assessment of multi-phase fuel under actual ambient conditions.

1. INTRODUCTION

Al powder with high burning rate and high energy density has been widely used in compound explosives, propellant, and fuel−air explosive (FAE). In the production process of solid−liquid mixture FAE, Al powder as a common metal component is often exposed to liquid fuel and volatile fuel vapor, which brings multi-phase explosion dangers.

Recently, many studies had conducted about the explosion performance of gas fuels,[1−4] liquid fuels,[5−7] and organic or metal dust.[8−10] For Al powder, Jin et al.[11] studied the laser-induced ignition and combustion characteristics between nano-sized aluminum and micron-sized aluminum powder and found that ignition delay time of nano-Al was much lower than that of micro-Al. Li et al.[12,13] investigated the explosion severity, flame propagation properties, and minimum ignition temperatures of micro-sized aluminum dust. For Al powder−liquid fuel mixtures, Liu et al.[14] studied the lower flammability limit (LFL) of Al powder−volatile liquid fuel mixtures in air. Yao et al.[15] studied the effect of concentration, component proportion, and ignition energy on the explosion performance of the aluminum dust−diethyl ether−air mixture.

The mixture of fuel−dust and the surrounding air is the prerequisite for the multi-phase explosion, and the air condition is greatly influenced by ambient pressure, temperature, and humidity. Mitu and Brandes[16,17] studied the explosion performance of methanol−air and ethanol−air mixtures under different ambient pressures and temperatures in closed spherical vessels. Blais et al.[18] studied the effect of initial reactant temperature on flame speeds in aluminum dust suspensions and found that the flame speed in aluminum−air mixtures increases by less than two times with an increase in temperature to about 524 K. Ma et al.[19] studied the spontaneous combustion characteristics of coal under different air humidity and found that humidity had effects on the crossing point temperature. Grabarczyk et al.[20] and Cammarota et al.[21] investigated the explosion pressure of isooctane, toluene, methano, and n-dodecane and summarized the effect of the initial temperature and pressure. For solid−liquid fuel mixtures, Sanchirico et al.[22] studied the effect of initial pressure

on the lower explosion limit of the nicotinic acid−acetone mixture. In our past work,[23−26] the explosion characteristics of diethyl ether, epoxypropane, n-pentane, and Al powder−liquid fuel under different ambient conditions were tested, and the influence mechanism of ambient parameters was discussed. However, most of the studies focused on the effect of single ambient parameter. In the actual plateau area, low ambient pressure was often accompanied by low temperature. Similarly, high temperatures are often accompanied by high humidity in rainy summer or tropical rainy climate section. Ambient temperature, pressure, and humidity were mutually affected. The explosion characteristics of fuel under binary ambient conditions could provide a basis for the assessment of explosion power and risk under actual ambient conditions.

In this study, the low-temperature (263−293 K) and low-pressure (101.3−57.4 kPa) as well as high-temperature (293−313 K) and high-humidity (48.3−90%) ambient conditions were simulated in the 20 L explosion vessel. The explosion pressure, maximum pressure rise rates, and LFL of Al powder−liquid fuel mixtures (A−D and A−D−N) were tested under the different ambient conditions. The experimental method to obtain the explosion characteristics of Al powder−liquid fuel mixtures under binary ambient conditions was introduced, and the estimation formula for LFL of A−D and A−D−N mixtures was provided, which could further help in explosion performance assessment of the multi-phase fuel under different ambient conditions.

2. EXPERIMENTAL APPARATUS AND PROCEDURES

2.1. Materials. Diethyl ether (99.5%, AR) and nitromethane (99.5%, AR) were provided by Beijing Tongguang Fine Chemical Company. The fuel reagents were used as received. Al powder (99.9%, flake, $D_{50} = 14.28 \, \mu$m) was provided by Liaoning Jinhua Electromechanical Co. Ltd. The solid−liquid fuel mass ratios of A−D mixture (Al powder−diethyl ether) and A−D−N mixture (Al powder 45−diethyl ether 35.2−nitromethane 19.8) were 45:55.

2.2. Experimental Procedures. The explosion tests of Al powder−liquid fuel mixtures under different ambient conditions were conducted in a 20 L explosion vessel test system, which was composed of a typical 20 L steel sphere explosion vessel (as shown in Figure 1), a pneumatic piping system, an
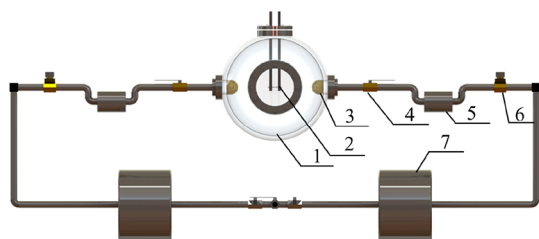
Figure 1. Experimental setup. (1) 20 L explosion vessel, (2) ignition electrodes, (3) sprayer, (4) ball valve, (5) sample cell (20 mL in volume), (6) solenoid valve, and (7) air reservoir.

ignition control system, a data acquisition system, and an ambient condition control system. The detailed information about the test system has been described in our past work.[23−26]

In a typical test, the internal ambient temperature, pressure, and humidity of the explosive vessel were adjusted by the ambient condition control system (low-temperature coolant circulating pump, a self-made heating mantle, a vacuum pump,

and an atomizing humidifier). When the required ambient parameters reached, Al powder and liquid fuels were mixed first and then added into the two sample cells. Then, the air compressor was turned on until the pressure in the air reservoirs reached 0.4 MPa. The solenoid valves were turned on, then the high-pressure gas carried the mixed fuel from the sample cell to the explosion vessel to form dust−mist−gas mixtures. Turn on the data acquisition system, and set the sampling frequency to MHz·s^{-1} of the pressure sensors with a sampling time of 1 s. Then, the mixtures with the energy of 90 J were ignited, and the explosion pressure data was collected. The typical time evolution curves of pressure during explosion under normal ambient condition are shown in Figure 2.
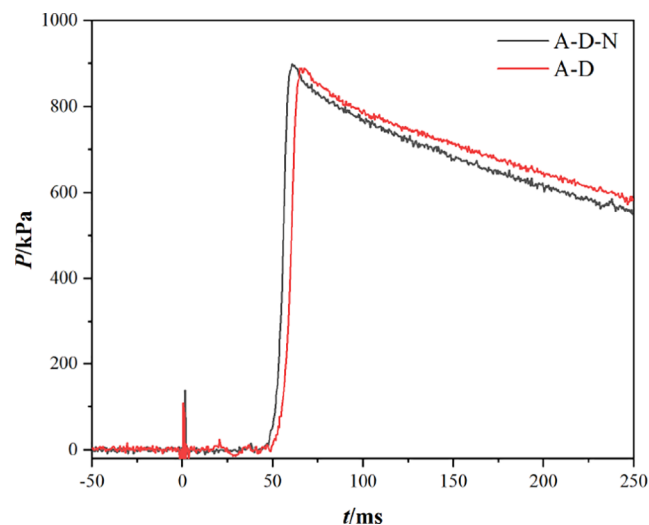
Figure 2. Typical time evolution curves of pressure during explosion.

The low temperature (263−293 K) and low pressure (101.3−57.4 kPa) as well as high temperature (293−313 K) and high humidity (48.3−90%) were selected test ambient conditions. The relative humidity in this study referred to the percentage of the vapor pressure in the air compared with the saturated vapor pressure at the same temperature. In a typical low-temperature and low-pressure test, first, the temperature is reduced in the explosion vessel using the low-temperature coolant circulating pump. Second, the pressure in the explosion vessel is reduced using the vacuum pump with the ball valves closed (avoiding the loss of mixture fuel). Finally, the ball valves were opened and ignited. At the beginning of a typical high-temperature and high-humidity test, first, the temperature is increased in the explosion vessel using the self-made heating mantle. Second, the atomizing humidifier is filled with hot water according to the temperature in the explosion vessel, and the vessel was moisturized.

3. RESULTS AND DISCUSSION

3.1. Explosion Pressure under Low Pressures and Low Temperatures. The explosion performance of the A−D and A−D−N mixtures with the mass concentrations of 450 g·m^{-3} was tested under low-temperature and low-pressure ambient conditions, and the explosion pressure results are shown in Figure 3. Under the same ambient pressures, the explosion pressure of fuel−air mixtures increased first and then decreased with the decreasing ambient temperature. Compared with gaseous state fuel, liquid state fuel had a larger explosion
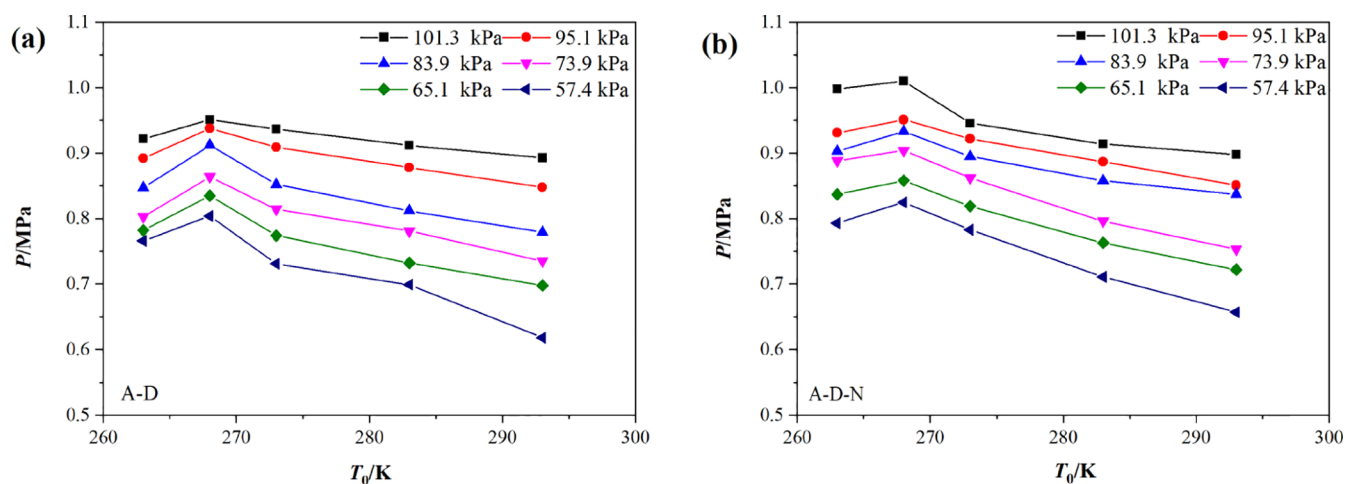
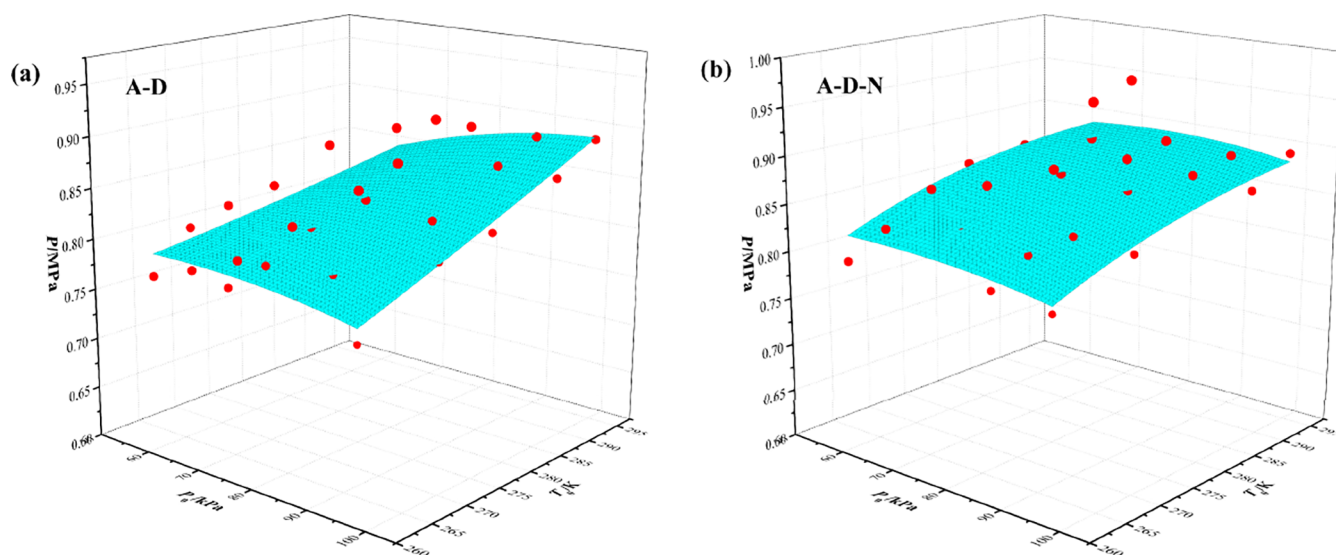**Figure 3.** Explosion pressure under low-temperature and low-pressure conditions for A−D (a) and A−D−N (b).

Figure 4. Fitting surface of explosion pressure with the initial ambient pressure and temperature for A−D (a) and A−D−N (b).
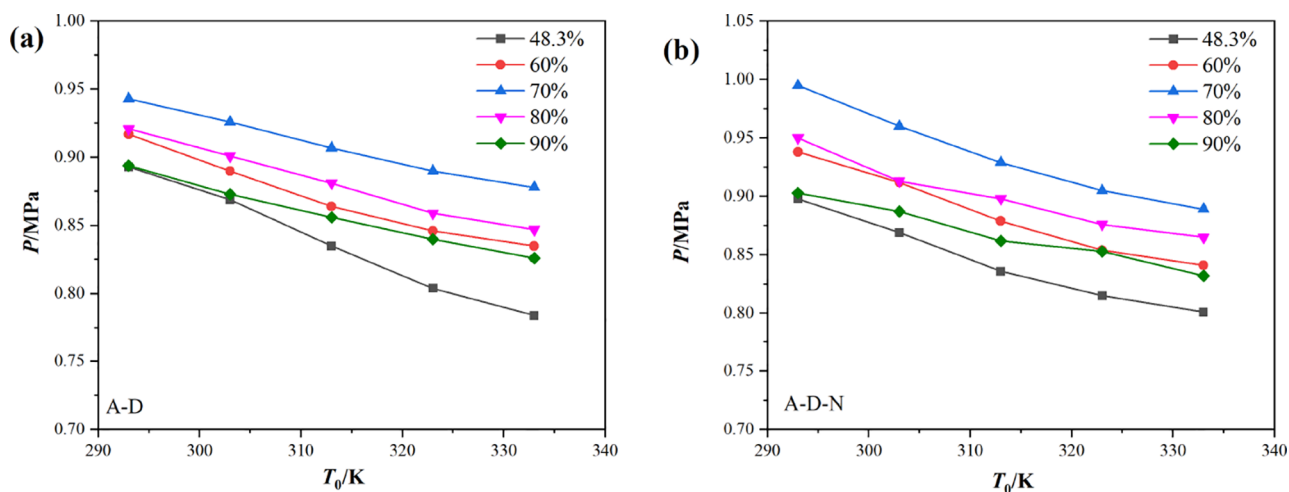

Figure 5. Explosion pressure under high-temperature and high-humidity conditions for A−D (a) and A−D−N (b).

pressure,[23,27] the content liquid state diethyl ether in the explosion vessel was increased with the decreasing ambient temperature, which resulted in the increasing explosion pressure. However, the lower ambient temperature was also associated with low reaction degree, resulting in the incomplete explosion reaction. When the ambient temperature was below 268 K, the explosion pressure began to decrease gradually. Under the same ambient temperatures, the explosion
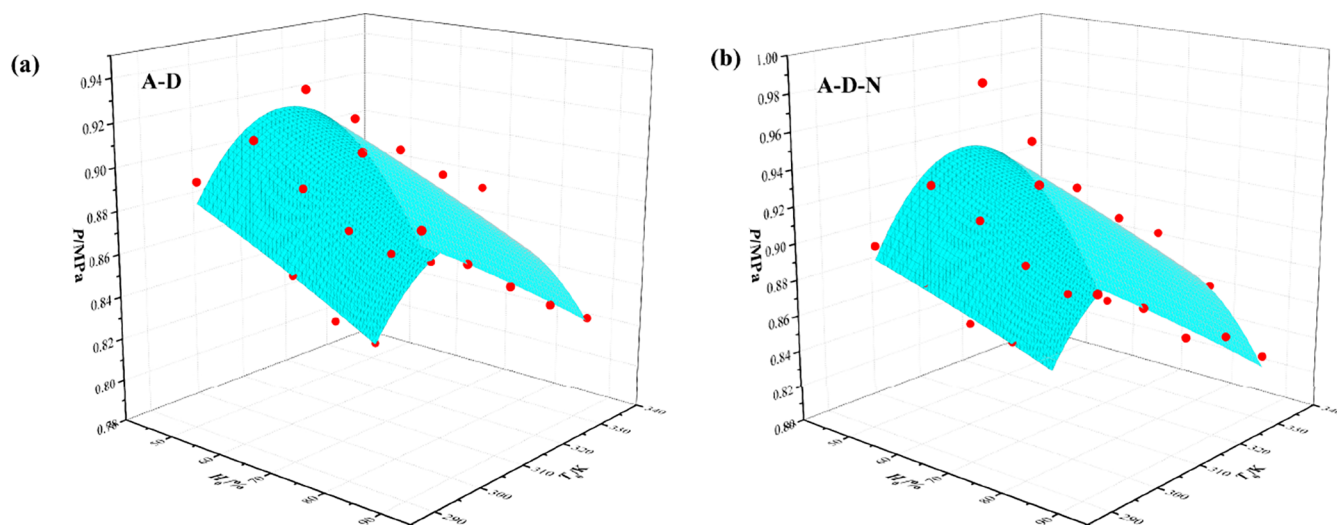
Figure 6. Fitting surface of explosion pressure with the initial ambient humidity and temperature for A−D (a) and A−D−N (b).
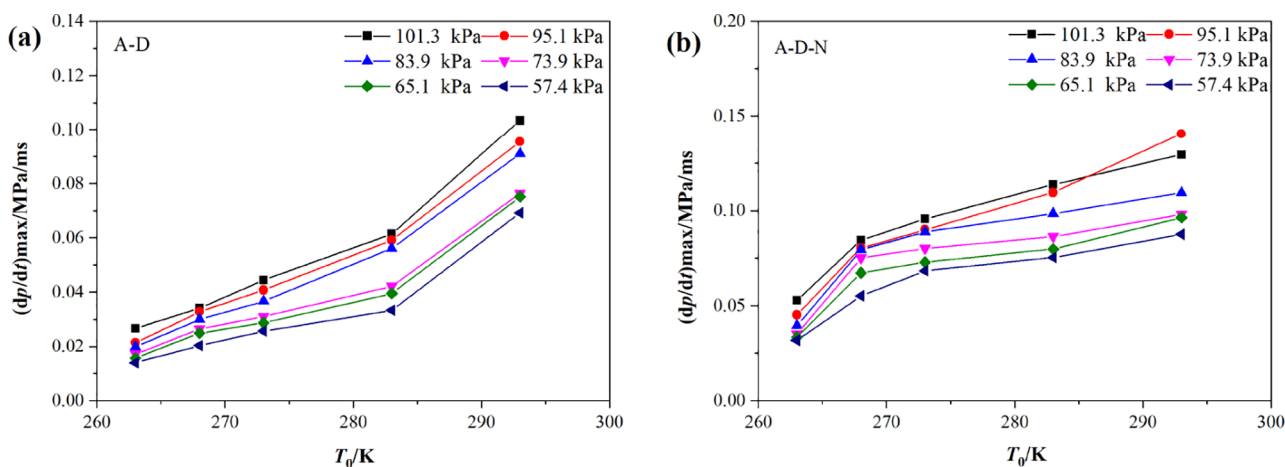

Figure 7. $(dp/dt)_{max}$ under low-temperature and low-pressure conditions for A−D (a) and A−D−N (b).

pressure of the fuel−air mixture was decreased with the decreasing ambient pressure. The lower ambient pressure was associated with low oxygen concentrations, resulting in the incomplete explosion reaction and low explosion pressure.

The variations of explosion pressure from 57.4 kPa to 101.325 kPa gradually reduced with the decreasing ambient temperature. The lower the ambient temperature, the smaller the variation of the explosion pressure with the ambient pressure. The lower the ambient pressure, the greater the explosion pressure varied with the ambient temperature. The A−D−N mixture had a smaller explosion pressure distribution variation from 263 K to 293 K than that of the A−D mixture, which indicated that the explosion pressure of the A−D−N mixture had a lower sensitivity to the variation of ambient temperature.

The relation fitting surface of explosion pressure with the ambient pressure and temperature can be obtained by Origin software, as shown in Figure 4a,b. The fitted surface relationship could estimate the explosion pressure of the A−D and A−D−N mixtures in the plateau section within a certain error range.

3.2. Explosion Pressure under High Temperature and High Humidity. The explosion performance of the A−D and A−D−N mixtures with the mass concentrations of 450 g·m^{-3}

were tested under high-temperature and high-humidity ambient conditions, and the explosion pressure results are shown in Figure 5. Under the same humidity, the explosion pressure of the fuel−air mixtures decreased gradually with the increasing ambient temperature. On the one hand, the content liquid state diethyl ether in the explosion vessel was decreased with the increasing ambient temperature. On the other hand, the density for the burning charge was decreased with the increasing ambient temperature,[28] which also caused a lower explosion pressure. Under the same ambient temperature, the explosion pressure of the fuel−air mixtures increased first and then decreased with the increase in ambient humidity. The explosion reaction of Al powder could be promoted by increasing the ambient humidity appropriately due to the generation of H_2. However, when humidity was over 70%, excess water vapor inhibited the explosion reaction.

The variations of explosion pressure from 48.3% to 90% gradually reduced with the decreasing ambient temperature. The lower the ambient temperature, the smaller the variation of the explosion pressure with the relative humidity. The lower the relative humidity, the greater the explosion pressure varied with the ambient temperature. The explosion pressure of the A−D−N mixture had a smaller distribution variation from 333 K to 293 K, which also indicated that the A−D−N mixture had
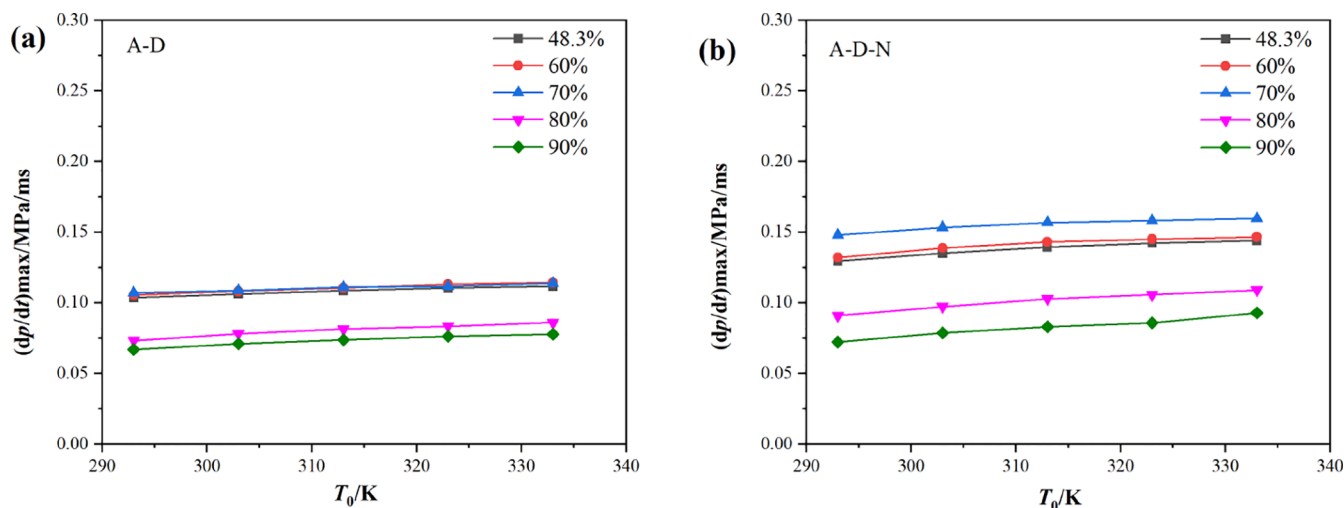
Figure 8. $(dp/dt)_{max}$ under high-temperature and high-humidity conditions for A−D (a) and A−D−N (b).
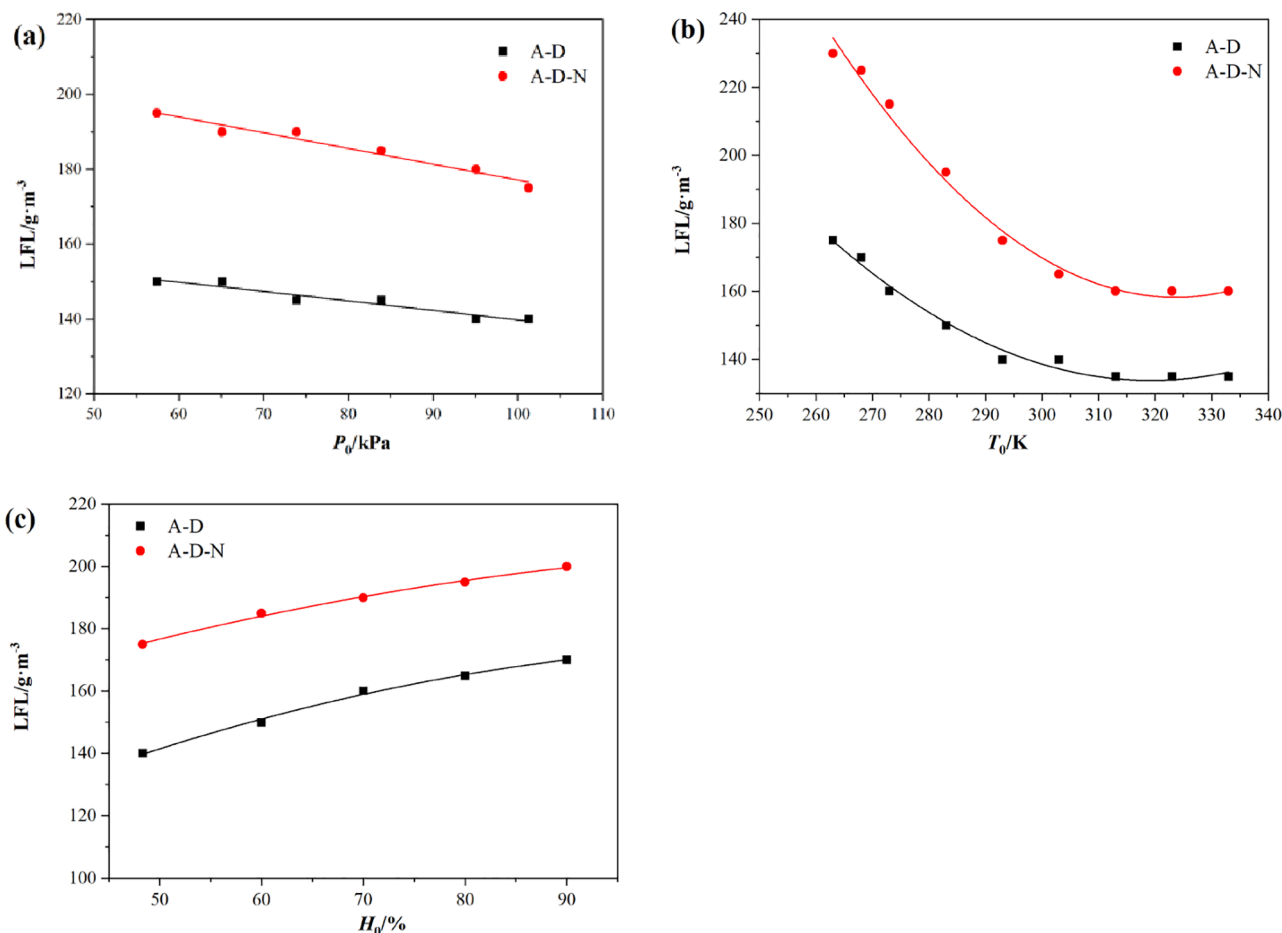

Figure 9. LFLs under different ambient (a) pressure, (b) temperature, and (c) humidity.

lower explosion pressure sensitivity to the variation of ambient temperature.

The relation fitting surface of explosion pressure with ambient temperature and humidity can be obtained, as shown in Figure 6a,b. The fitted surface relationship could estimate the explosion pressure of A−D and A−D−N mixtures in rainy summer or tropical rainy climate section within a certain error range.

3.3. Explosion Pressure Rise Rate. The explosion pressure rise rate showed the explosion reaction rates of the mixture fuels. Then, the maximum explosion pressure rise rates of A−D and A−D−N mixtures at the different test conditions are shown in Figures 7 and 8. As shown in Figure 7, the maximum pressure rise rates of the A−D and A−D−N mixtures decreased with decreasing initial ambient pressures and temperatures. With the increase in ambient temperature, the content of gaseous diethyl ether was increased, and the

Table 1. Polynomial Fitting Curve Results of the LFLs

samples	parameters	polynomial fitting curves	R^2
A–D	P_0	LFL = $-0.234P_0 + 164.36$	0.932
	T_0	LFL = $0.013T_0^2 - 8.28T_0 + 1455.54$	0.987
	H_0	LFL = $-0.008H_0^2 + 1.836H_0 + 69.72$	0.996
A–D–N	P_0	LFL = $-0.421P_0 + 219.28$	0.959
	T_0	LFL = $0.021T_0^2 - 13.453T_0 + 2335.02$	0.991
	H_0	LFL = $-0.005H_0^2 + 1.328H_0 + 123.79$	0.996

contact between gas–liquid–solid fuel molecules was more comprehensive, which was beneficial to increase the explosion reaction rate. With the decrease in ambient pressure, the oxygen content decreased, the explosion reaction rate decreased. As shown in Figure 8, with the increase in humidity, the explosion pressure increased first and then decreased due to the generation of H_2 and the inhibition of excess water vapor.

3.4. Lower Flammability Mass Concentration Limits. The lower flammability mass concentration limits (LFL) of the Al powder–liquid fuel mixtures could be defined as the lowest mass concentration, which could be ignited under the ignition energy of 90 J. The concentration interval adopted in the LFL tests was 5 g·m^{-3}. The upper flammability mass concentration limits (UFLs) of the Al powder–liquid fuel mixtures were over 1000 g·m^{-3}, which were nearly the volume limits of the sample cell. Then, the UFLs of the Al powder–liquid fuel mixtures were not examined in this study.

The LFLs of the Al powder–liquid fuel mixtures under different initial ambient conditions are shown in Figure 9a–c, and were increased with the decreasing ambient pressures and temperatures as well as the increasing humidity. The LFLs were mainly influenced by the content of O_2 and gaseous diethyl ether. With the decreasing ambient pressure, the gaseous fuel content increased, the O_2 content decreased, then the LFL increased. With the decreasing ambient temperature, gaseous diethyl ether obviously decreased, and the LFL increased. With the increasing relative humidity, water vapor also absorbed the energy of ignition and chemical reaction, inhibiting the explosion reaction and increasing the LFLs. Under the same initial ambient condition, A–D mixture had a lower LFL than that of A–D–N mixture due to the higher content of gaseous diethyl ether. On the one hand, nitromethane could dissolve part of diethyl ether and reduce the content of gaseous diethyl ether. On the other hand, nitromethane has a high vaporization temperature (100–102 °C), and the vaporization of nitromethane could be ignored during the mixing process. The ambient parameters tested in this study relatively influenced the LFLs in the order: ambient temperature > relative humidity > ambient pressure.

After polynomial fitting of curves in Figure 9a–c, the mathematical model of the LFLs of the Al powder–liquid fuel mixture with environmental parameters within the range of test ambient conditions could be obtained. The corresponding polynomial fitting equation and correlation coefficient are shown in Table 1. The correlation coefficients of the LEL fitting curves of fuel–air mixtures with respect to ambient pressure P_0 were relatively low, especially the A–D mixtures, because the 5 g·m^{-3} concentration interval was not accurate enough to distinguish LELs at low ambient pressure. The fitted mathematical relationship could estimate the LFLs of the A–D and A–D–N mixtures within a certain error range under different initial ambient conditions.

In order to figure out the influence of different ambient parameters, the LFLs under low-temperature and low-pressure (73.9 kPa) as well as high-temperature and high-humidity (70%) ambient conditions were tested, and the results are shown in Figure 10. Under the same ambient temperature, the
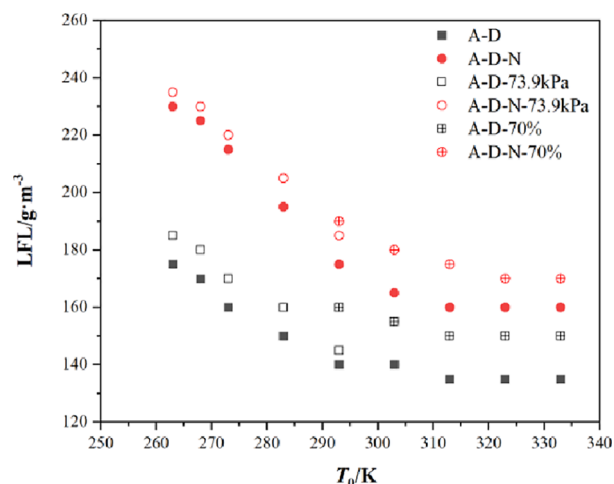

Figure 10. LFLs under different binary initial ambient conditions.

LFLs under 73.9 kPa were higher than that under 101.325 kPa, and the LFLs under 70% were higher than that under 48.3%. The A–D–N mixture had a lower LFL sensitivity to ambient pressure and humidity, while the A–D mixture had a lower LFL sensitivity to the variation of ambient temperature. Ambient pressure and humidity made little difference on the LFL variation of the mixtures with different ambient temperatures.

4. CONCLUSIONS

The explosion pressure, maximum explosion pressure rise rates, and lower flammability mass concentration limits of A–D and A–D–N were investigated under low-temperature and low-pressure as well as high-temperature and high-humidity initial ambient conditions in the 20 L explosion vessel. The main conclusions are as follows:

(1) The lower the ambient temperature, the smaller the variation of the explosion pressure with the ambient pressure and relative humidity. The lower the ambient pressure and relative humidity, the greater the explosion pressure varied with the ambient temperature.

(2) The ambient pressure and humidity made little difference on the LFL variation of the fuel mixtures than ambient temperatures.

(3) The explosion pressure of the A–D–N mixtures had a lower sensitivity to ambient temperature than that of the A–D mixtures.

The experimental result could further help in explosion performance and risk assessment of the multi-phase fuel under actual ambient conditions. In order to improve the prevention of multi-phase fuel explosion in industrial production, it is necessary to further study the multi-phase explosion mechanism and explosion resistance technology.

■ AUTHOR INFORMATION

Corresponding Author

Jian Yao − *School of Mechanical Engineering, Nanjing University of Science and Technology, Jiangsu, Nanjing 210094, P. R. China;* ⊙ orcid.org/0000-0003-3525-2075; Email: yaojian1991@njust.edu.cn

Authors

Chunhua Bai − *State Key Laboratory of Explosion Science and Technology, Beijing Institute of Technology, Beijing 100081, P. R. China*

Chi Zhang − *State Key Laboratory of Explosion Science and Technology, Beijing Institute of Technology, Beijing 100081, P. R. China*

Complete contact information is available at:
https://pubs.acs.org/10.1021/acsomega.2c03970

Notes

The authors declare no competing financial interest.

■ REFERENCES

(1) Cao, W.; Zhou, Z.; Li, W.; Zhao, Y.; Yang, Z.; Zhang, Y.; Ouyang, S.; Shu, C.; Tan, Y. Under-Expansion Jet Flame Propagation Characteristics of Premixed H_2/Air in Explosion Venting. *Int. J. Hydrogen Energy* **2021**, *46*, 38913−38922.

(2) Cao, W.; Zhou, Z.; Zhou, W.; Xu, S.; Xiao, Q.; Cao, W.; Jiao, F.; Zhang, Y.; Yu, S.; Xu, S. The Flow Field Behaviours of Under-Expansion Jet Flame in Premixed Hydrogen/Air Explosion Venting. *Int. J. Hydrogen Energy* **2022**, *47*, 10420−10430.

(3) Zhang, B.; Liu, H. The Effects of Large Scale Perturbation-Generating Obstacles on the Propagation of Detonation Filled with Methane-Oxygen Mixture. *Combust. Flame* **2017**, *182*, 279−287.

(4) Zhang, B.; Li, Y.; Liu, H. Ignition Behavior and the Onset of Quasi-Detonation in Methane-Oxygen Using Different End Wall Reflectors. *Aerosp. Sci. Technol.* **2021**, *116*, 106873.

(5) Cheng, Y.; Hu, E.; Deng, F.; Yang, F.; Zhang, Y.; Tang, C.; Huang, Z. Experimental and kinetic comparative study on ignition characteristics of 1-pentene and n-pentane. *Fuel* **2016**, *172*, 263−272.

(6) Cheng, Y.; Hu, E.; Lu, X.; Li, X.; Gong, J.; Li, Q.; Huang, Z. Experimental and Kinetic Study of Pentene Isomers and N-pentane in Laminar Flames. *Proc. Combust. Inst.* **2017**, *36*, 1279−1286.

(7) Bai, C.; Liu, N.; Zhang, B. Experimental investigation on the lower flammability limits of diethyl ether/ n-pentane/epoxypropane-air mixtures. *J. Loss Prev. Process Ind.* **2019**, *57*, 273−279.

(8) Cao, W.; Qin, Q.; Cao, W.; Lan, Y.; Chen, T.; Xu, S.; Cao, X. Experimental and Numerical Studies on the Explosion Severities of Coal Dust/Air Mixtures in a 20-L Spherical Vessel. *Powder Technol.* **2017**, *310*, 17−23.

(9) Wang, Q.; Fang, X.; Shu, C.; Wang, Q.; Sheng, Y.; Jiang, J.; Sun, Y.; Sheng, Z. Minimum Ignition Temperatures and Explosion Characteristics of Micron-Sized Aluminium Powder. *J. Loss Prev. Process Ind.* **2020**, *64*, 104076.

(10) Di Sarli, V.; Sanchirico, R.; Benedetto, A. On the Effect of Initial Pressure on the Minimum Explosive Concentration of Dust in Air. *Powder Technol.* **2018**, *336*, 567−572.

(11) Jin, X.; Li, S.; Yang, Y.; Huang, X. Comparison on Laser Ignition and Combustion Characteristics of Nano- and Micron-Sized Aluminum. *Combust. Sci. Technol.* **2021**, *193*, 341−353.

(12) Li, Q.; Wang, K.; Zheng, Y.; Mei, X.; Lin, B. Explosion Severity of Micro-Sized Aluminum Dust and Its Flame Propagation Properties in 20 L Spherical Vessel. *Powder Technol.* **2016**, *301*, 1299−1308.

(13) Li, Q.; Zhang, G.; Zheng, Y.; Liu, J.; Li, X. Investigation on the Correlations between Thermal Behaviors and Explosion Severity of Aluminum Dust/Air Mixtures. *Powder Technol.* **2019**, *355*, 582−592.

(14) Liu, N.; Bai, C.; Yao, N.; Yao, J. Experimental Investigation of the Lower Flammability Limit of Volatile Liquid Fuel-Aluminum Powder Mixtures in air. *J. Loss Prev. Process Ind.* **2020**, *66*, 104160.

(15) Yao, N.; Bai, C.; Wang, L.; Liu, N. Investigation on the Explosion Characteristics of an Aluminum Dust-Diethyl Ether-Air Mixture. *ACS Omega* **2021**, *6*, 18868−18875.

(16) Mitu, M.; Brandes, E. Explosion Parameters of Methanol-Air Mixtures. *Fuel* **2015**, *158*, 217−223.

(17) Mitu, M.; Brandes, E. Influence of Pressure, Temperature and Vessel Volume on Explosion Characteristics of Ethanol/Air Mixtures in Closed Spherical Vessels. *Fuel* **2017**, *203*, 460−468.

(18) Blais, F.; Julien, P.; Palecka, J.; Goroshin, S.; Bergthorson, M. Effect of Initial Reactant Temperature on Flame Speeds in Aluminum Dust Suspensions. *Combust. Sci. Technol.* **2020**, *194*, 1513−1526.

(19) Ma, D.; Qin, B.; Song, S.; Liang, H.; Gao, A. An Experimental Study on the Effects of Air Humidity on the Spontaneous Combustion Characteristics of Coal. *Combust. Sci. Technol.* **2017**, *189*, 2209−2219.

(20) Grabarczyk, M.; Teodorczyk, A.; Di Sarli, V.; Di Benedetto, A. Effect of Initial Temperature on the Explosion Pressure of Various Liquid Fuels and Their Blends. *J. Loss Prev. Process Ind.* **2016**, *44*, 775−779.

(21) Cammarota, F.; Di Benedetto, A.; Di Sarli, V.; Salzano, E. Influence of Initial Temperature and Pressure on the Explosion Behavior of N-dodecane/air Mixtures. *J. Loss Prev. Process Ind.* **2019**, *62*, 103920.

(22) Sanchirico, R.; Di Sarli, V.; Di Benedetto, A. Effect of Initial Pressure on the Lower Explosion Limit of Nicotinic Acid/Acetone Mixture. *J. Loss Prev. Process Ind.* **2020**, *64*, 104075.

(23) Bai, C.; Liu, W.; Yao, J.; Zhao, X.; Sun, B. Explosion Characteristics of Liquid Fuels at Low Initial Ambient Pressures and Temperatures. *Fuel* **2020**, *265*, 116951.

(24) Yao, J.; Zhang, C.; Liu, W.; Bai, C.; Zhao, X.; Sun, B..; Liu, N. The Explosion Characteristics of Diethyl Ether-Al Mixtures under Different Ambient Conditions. *Combust. Flame* **2021**, *227*, 162−171.

(25) Bai, C.; Zhang, C.; Liu, W.; Zhao, X.; Sun, B.; Yao, J. Effect of Nitromethane on Fuel/Air Explosion Characteristics under Different Ambient Conditions. *Combust. Flame* **2021**, *234*, 111632.

(26) Zhang, C.; Bai, C.; Ren, J.; Chang, C.; Yao, J. The Promotion of Nitromethane on Solid-Liquid Fuel/Air Mixtures Explosion Characteristics under Different Ambient Conditions. *Fuel* **2022**, *322*, 124190.

(27) Hayashi, S.; Kumagai, S. Flame Propagation in Fuel Droplet-Vapor-Air Mixtures. *Symp. Combust.* **1975**, *15*, 445−452.

(28) Razus, D.; Brinzea, V.; Mitu, M.; Oancea, D. Temperature and Pressure Influence on Explosion Pressures of Closed Vessel Propane-Air Deflagrations. *J. Hazard. Mater.* **2010**, *174*, 548−555.